Numerical Evidence for Critical Behavior of the Two-Dimensional Nonequilibrium Zero-Temperature Random Field Ising Model

Djordje Spasojević, Sanja Janićević, and Milan Knežević
Faculty of Physics, University of Belgrade, POB 368, 11001 Belgrade, Serbia
(Received 18 November 2010; revised manuscript received 27 December 2010; published 25 April 2011)

We give numerical evidence that the two-dimensional nonequilibrium zero-temperature random field Ising model exhibits critical behavior. Our findings are based on the results of scaling analysis and collapsing of data, obtained in extensive simulations of systems with sizes sufficiently large to clearly display the critical behavior.

DOI: 10.1103/PhysRevLett.106.175701 PACS numbers: 64.60.Ht, 75.40.Mg, 75.50.Lk, 75.60.Ej

During the past three decades, the random field Ising model (RFIM) has been intensely studied [1,2] as a model for cooperative behavior in magnets with quenched disorder. A particular line of research was on the disorder-induced phase transition in the zero-temperature version of RFIM [3], due to its conceptual importance and relevance for interpretation of Barkhausen noise data [4].

Renormalization-group and numerical studies [5,6] of nonequilibrium zero-temperature RFIM revealed a nontrivial critical behavior for system dimensions $2 < d < 6$, and mean-field criticality [7] for $d \geq 6$. Gradually, many similarities with the criticality of equilibrium zero-temperature RFIM [8] were observed, leading ultimately to the conclusion that both models are very likely to be in the same universality class [9] for $d \geq 3$. However, despite considerable effort [10], the important question about the criticality of the nonequilibruim model in 2D remained unresolved [2], which motivated us to reconsider the problem.

In this Letter we give numerical evidence for the critical behavior of the nonequilibrium zero-temperature random field Ising model in two dimensions. The model treats a system of Ising spins $S_i = \pm 1$ located at a square lattice of size L with periodic boundary conditions. The nearest neighbor $\langle i, j \rangle$ spins are ferromagnetically coupled with strength J. Besides, each spin experiences a uniform external magnetic field H, and a quenched local random field h_i. Thus, the RFIM Hamiltonian is $\mathcal{H} = -J\sum_{\langle i,j \rangle} S_i S_j - H\sum_i S_i - \sum_i h_i S_i$, while the effective field acting on the spin S_i is $h_i^{\text{eff}} = J\sum_j S_j + H + h_i$. In what follows, we take $J = 1$.

While its sign is equal to the sign of h_i^{eff} the spin S_i is stable—otherwise, it flips. This rule defines the dynamics of the nonequilibrium model when the system is driven by an increase of H from $-\infty$ (and all spins are -1) to $+\infty$ (when all spins are $+1$). We consider only the adiabatic regime: H is increased so as to trigger only the least stable spin, and then kept constant until all spins become stable.

The system evolution depends on the local quenched field. Its values h_i at different lattice sites are chosen randomly and independently from some zero-mean distribution $\rho(h)$, so $\langle h_i \rangle = 0$ and $\langle h_i h_j \rangle = 0$. Here we use a Gaussian distribution $\rho(h) = \frac{1}{\sqrt{2\pi}R} \exp(-\frac{h^2}{2R^2})$ whose standard deviation R quantifies disorder in the system.

We report that in the 2D case, as in higher dimensions, a critical disorder R_c exists. It separates two different regimes—see Fig. 1: for $R > R_c$ the magnetization curve $M_R(H)$ is a smooth function of H, while for $R < R_c$ a majority of spins flip in a single system-spanning avalanche, causing a jump in magnetization. For $R = R_c$, the magnetization curve is still smooth, but has an infinite slope $dM_{R_c}(H)/dH$ at the critical field H_c.

Near the critical point (R_c, H_c), magnetization scales as [2,6]

$$m_R(H) \sim |r|^{\beta} \mathcal{M}_{\pm}(h'/|r|^{\beta\delta}), \tag{1}$$

implying that the scaled quantities $m_R(H)/|r|^{\beta}$, plotted against $h'/|r|^{\beta\delta}$, fall onto a single curve: $\mathcal{M}_{+}(h'/|r|^{\beta\delta})$

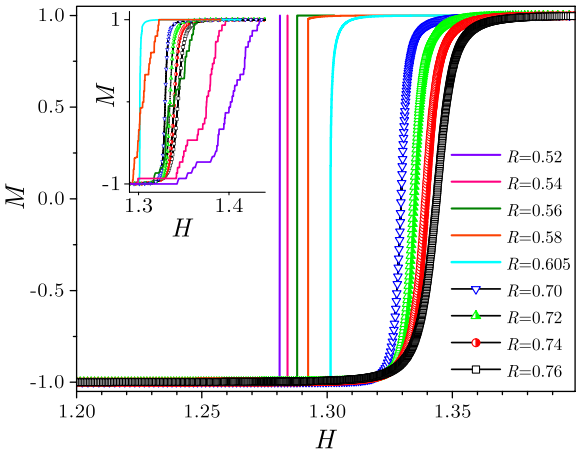

FIG. 1 (color online). Magnetization curves $M_R(H)$ for disorders $R = 0.52 - 0.76$ and system size $L = 131\,072$ for which $R_c^{\text{eff}} = 0.605$—see Eq. (10). For $R < R_c^{\text{eff}}$, the value H_{sp} of external magnetic field at which spanning avalanche occurs varies with random field configuration (RFC). Main panel: magnetization curves for single RFC sorted in increasing disorder R. Inset: magnetization curves averaged over 30 RFC; while this number is small, steps (which appear due to spanning avalanches and stochastic distribution of H_{sp}) are visible.

for $R > R_c$ [and $\mathcal{M}_-(h'/|r|^{\beta\delta})$ for $R < R_c$]. Here, $m = M_R(H) - M_c$, where $M_c = M_{R_c}(H_c)$ is the critical magnetization, $r = (R - R_c)/R$ is a reduced disorder, and $h' = H - H_c - br$ is a reduced magnetic field "rotated" by parameter b in order to compensate the change of $H_c^{\rm eff}(r) \approx H_c + br$ with (small) r; here, $H_c^{\rm eff}(r)$ is the effective critical field, i.e., the value of H at which the susceptibility $\chi_R(H) = dM/dH$ attains its maximum value as a function of H for given R [6]. Finally, $\mathcal{M}_\pm$ are universal scaling functions of a single variable, while β and δ are the critical exponents that pertain to scaling $\Delta M \sim |r|^\beta$ of magnetization jump ΔM below R_c, and to scaling $m \sim h'^\delta$ at R_c, respectively. Because of (1)

$$\chi_R(H) \sim |r|^{\beta-\beta\delta}\,\mathcal{M}'_\pm(h'/|r|^{\beta\delta}), \tag{2}$$

implying an analogous collapse of data onto derivatives $\mathcal{M}'_\pm(x) = d\mathcal{M}_\pm(x)/dx$ of scaling functions $\mathcal{M}_\pm(x)$.

To achieve collapsing, we have developed and used an algorithm that minimizes the width w of the region that contains collapsing data [11] without any assumption about analytical form of the underlying scaling function; for a similar algorithm, see [12].

In the main panel of Fig. 2 we present the collapse of magnetization according to (1), and in the inset we give the collapse of susceptibility according to (2); the values of universal exponents β and $\beta\delta$, and nonuniversal quantities R_c, H_c, M_c, and b are given in Table I. The collapses look better than those obtained for $d \geq 3$ and in the mean-field model—cf. [6,10]. For the integrated avalanche size distributions, the case is different.

The avalanche size distribution $D_{R,H}(S)$ for avalanches triggered at the external magnetic field H scales with avalanche size S (i.e., the number of spins flipped) as [2,6]

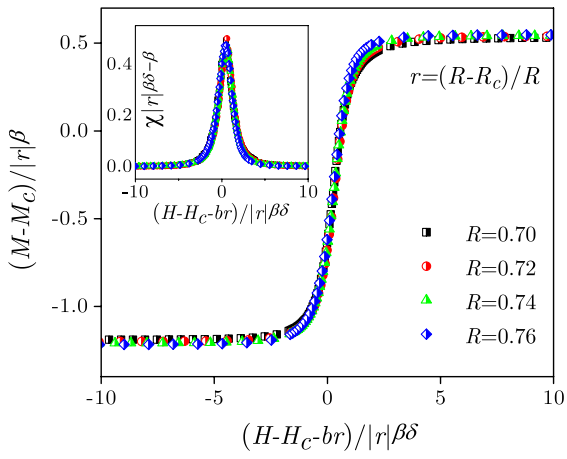

FIG. 2 (color online). Scaling collapse of magnetization M (main panel) and susceptibility χ curves (inset) for disorders $R = 0.70$–0.76 and system size $L = 131\,072$. The curves are averages of 30 random field configurations for each R. Collapsing parameters: $\beta = 0.15$, $\beta\delta = 4.8$, $R_c = 0.54$, $H_c = 1.275$, $M_c = 0$, and $b = 0.24$; for both collapses, the width (see [11]) is $w = 2.1 \times 10^{-2}$.

TABLE I. Universal critical exponents (top part) and nonuniversal scaling variables (bottom part) for 2D model. The quoted errors are based on Monte Carlo estimation and statistical uncertainties of the underlying data—see Chap. 15.6 in [13].

β	$\beta\delta$	τ	$\tau + \sigma\beta\delta$
0.15 ± 0.04	4.8 ± 0.2	1.54 ± 0.05	2.02 ± 0.06
σ	ν	$d + \beta/\nu$	η
0.10 ± 0.01	5.15 ± 0.20	2.04 ± 0.03	1.05 ± 0.06
R_c	H_c	M_c	b
0.54 ± 0.02	1.275 ± 0.020	0.00 ± 0.01	0.24 ± 0.04

$$D_{R,H}(S) \sim S^{-\tau}\mathcal{D}_\pm(S^\sigma|r|,\, h'|r|^{-\beta\delta}), \tag{3}$$

where $\mathcal{D}_\pm(X)$ are universal scaling functions. Therefore, the integrated avalanche size distribution $D_R^{(\rm int)}(S) = \int_{-\infty}^{+\infty} D_{R,H}(S)dH$ scales as

$$D_R^{(\rm int)}(S) \sim S^{-(\tau+\sigma\beta\delta)}\bar{\mathcal{D}}_\pm^{(\rm int)}(S^\sigma|r|), \tag{4}$$

where τ is the avalanche size exponent, while the cutoff exponent σ describes scaling of the largest avalanche size: $S_{\rm max} \sim |r|^{-1/\sigma}$.

For $R = R_c$ and for the infinite system, the expression (4) reduces to a pure power law $D_R^{(\rm int)}(S) \sim S^{-(\tau+\sigma\beta\delta)}$, which is expected to display clear scaling regions for finite systems and $R \approx R_c$ as well. This is illustrated in the bottom inset in Fig. 3, whence we see that only for sufficiently big systems the scaling region, increasing with L, can be distinguished from an unusually long initial region.

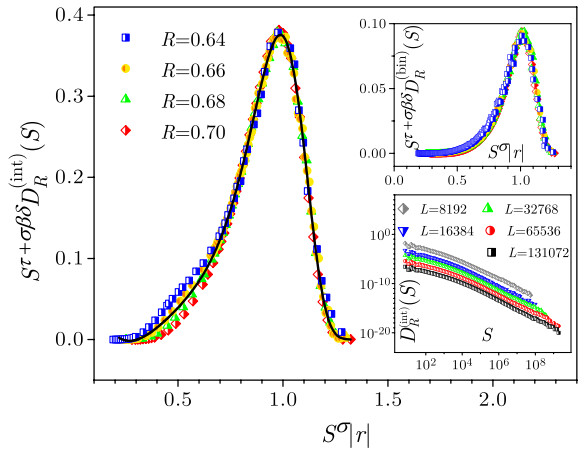

FIG. 3 (color online). Scaling collapse of integrated distributions $D_R^{(\rm int)}(S)$ of avalanche size S (symbols) for disorders $R = 0.64$–0.70 and system size $L = 65\,536$; $w = 4.5 \times 10^{-2}$. The curves are averages of 600 random field configurations for each R. The solid line represents the phenomenological curve (5). Collapsing of binned distributions $D_R^{(\rm bin)}(S)$ for the same simulation data is shown in the top inset; $w = 9.4 \times 10^{-3}$. In the bottom inset, integrated distributions $D_R^{(\rm int)}(S)$ of avalanche size S for system sizes $L = 8192 - 131\,072$ are shown. The graphs for $L < 131\,072$ are shifted up for better visibility.

Note that our largest lattice size (131072) far exceeds the "breakup length" $L_b \sim 10^4$ at $R_c = 0.54$ [14].

For $R > R_c$, the expression (4) also implies that the scaled quantities $D_R^{(\mathrm{int})}(S)S^{\tau+\sigma\beta\delta}$, plotted against $S^\sigma r$, should collapse onto a single curve—$\bar{\mathcal{D}}_+^{(\mathrm{int})}(S^\sigma r)$. The collapse is shown in Fig. 3 together with a phenomenological form [2,6]

$$\bar{\mathcal{D}}_+^{\mathrm{int}}(X) = e^{-0.608X^{1/\sigma}} \times (0.193 - 1.903X + 6.432X^2 - 8.929X^3 + 4.895X^4) \quad (5)$$

for the universal scaling function $\bar{\mathcal{D}}_+^{(\mathrm{int})}(X)$.

Although $D_R^{(\mathrm{int})}(S)$ curves collapse well for large avalanches, they show a noticeable branching for small sizes. The branching disappears for the binned distributions $D_{R,H_1,H_2}^{(\mathrm{bin})}(S) = \int_{H_1}^{H_2} D_{R,H}(S)dH$, provided the bins (H_1, H_2) are properly chosen. Thus, for $H_1 = H_c - r^{\beta\delta}\Delta H_0/2$ and $H_2 = H_c + r^{\beta\delta}\Delta H_0/2$, where $\Delta H_0 = H_2 - H_1$ is the bin width for $r = 0$, binned distributions $D_R^{(\mathrm{bin})}(S) \equiv D_{R,H_1,H_2}^{(\mathrm{bin})}(S)$ scale like the integrated distributions, and $D_R^{(\mathrm{bin})}(S)S^{\tau+\sigma\beta\delta}$ data, plotted against $S^\sigma r$, collapse—see the top inset in Fig. 3. The values of σ, and $\tau + \sigma\beta\delta$ are given in Table I, together with the value of τ obtained by fitting $D_{R,H}(S)$ to the power-law $D_{R,H}(S) \sim S^{-\tau}$.

For nonequilibrium RFIM near the critical point, the correlation function for avalanches at external field H scales as [2,6]

$$G_{R,H}(x) \sim \frac{1}{x^{d-2+\eta}} \mathcal{G}_\pm\left(\frac{x}{\xi(r, h')}\right), \quad (6)$$

where x is the distance between spins flipped in the same avalanche, η is the exponent called anomalous dimension, $\mathcal{G}_\pm$ are universal scaling functions, and ξ is the correlation length. For $h' = 0$ the correlation length ξ diverges when $r \to 0$. If power-law scaling applies, then $\xi(r, h') \sim |r|^{-\nu}\mathcal{Y}_\pm(h'/|r|^{-\beta\delta})$ for small h', where $\mathcal{Y}_\pm$ are the universal scaling functions. In this case

$$\xi \sim |r|^{-\nu} \quad (7)$$

for $h' = 0$, which is corroborated by our numerical data—see Fig. 4. The values of correlation length ξ were obtained from the fit of raw correlation data to the form

$$G_{R,H}(x) \sim \exp(-x/\xi)/x^{d-2+\eta}, \quad (8)$$

which also gives $\eta \approx 1$. The collapse of $G_{R,H}(x)x^{d-2+\eta}$ data against x/ξ is shown in Fig. 5.

A further consequence of scaling (6) is that the integral avalanche correlation function scales as [2,6]

$$G_R^{(\mathrm{int})}(x) \sim x^{-(d+\beta/\nu)}\bar{\mathcal{G}}_\pm(x|r|^\nu). \quad (9)$$

The corresponding collapse of data, presented in the top inset of Fig. 4, is obtained for the values of correlation length exponent ν and exponent combination $d + \beta/\nu$ given in Table I.

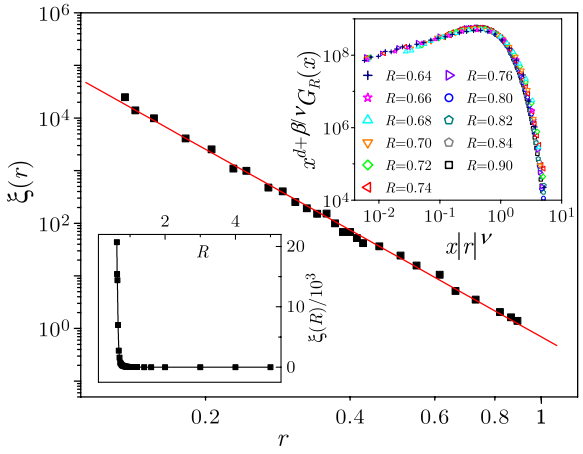

FIG. 4 (color online). Power-law divergence $\xi \sim |r|^{-\nu}$ of correlation length ξ with reduced disorder r for reduced magnetic field $h' = 0$. In the bottom inset, the same data are shown against R on a linear scale. Top inset: scaling collapse of correlation function $G_R^{(\mathrm{int})}(x)$ for disorders $R = 0.64$–0.90 and system size $L = 131\,072$; $w = 6.8 \times 10^6$. The curves are averages of 30 random field configurations for each R.

So far we have not discussed how the model data scale with system size L. For each system size L there exists an effective critical disorder $R_c^{\mathrm{eff}}(L)$ below which spanning avalanches appear [6]. The effective critical disorder $R_c^{\mathrm{eff}}(L)$ is greater than R_c, and $R_c^{\mathrm{eff}}(L) \to R_c$ when $L \to \infty$. It is expected that for $R = R_c^{\mathrm{eff}}(L)$ the correlation length should be of the order of the system's size, $\xi \sim L$. Hence, the power-law prediction (7), with reduced disorder $r = (R - R_c)/R$, implies

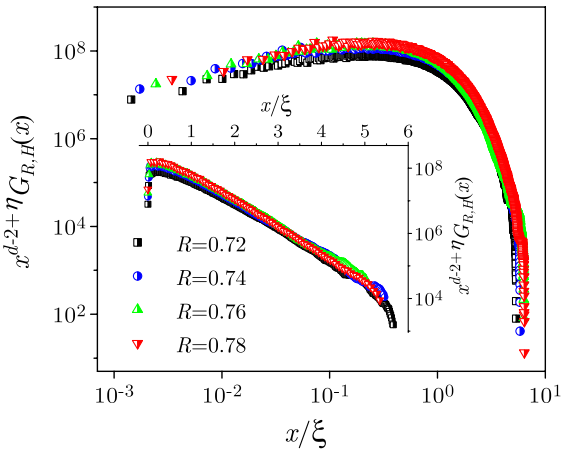

FIG. 5 (color online). Scaling collapse of the correlation function $G_{R,H}(x)$ for the avalanches at reduced field $h' = 0$. The collapse is obtained for $\eta = 1$ and correlation lengths from Fig. 4; $w = 4.6 \times 10^6$. Inset: the same collapse on the lin-log scale illustrates the applicability of approximation (8).

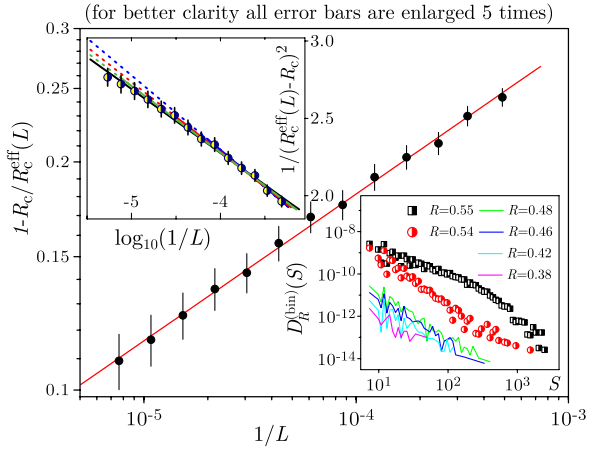

FIG. 6 (color online). Effective critical disorder $R_c^{\rm eff}(L)$ versus system size L (symbols) and the power-law prediction $[R_c^{\rm eff}(L) - R_c]/R_c^{\rm eff}(L) \sim L^{-1/\nu}$ (continuous line) with $R_c = 0.54$ and $\nu = 5.14$. Top inset: Bray-Moore scaling $\xi \sim e^{\tilde{a}/|R_c^{\rm eff}(L)-R_c|^2}$, $R_c \sim 0$; $\Delta R_c^{\rm eff}(L) = 0.001\,25$. Bottom inset: size distributions for $R = 0.38$–0.55, $L = 65\,536$, and more than 600 random field configurations for each R.

$$[R_c^{\rm eff}(L) - R_c]/R_c^{\rm eff}(L) \sim L^{-1/\nu}. \tag{10}$$

As can be seen from Fig. 6, our data are in agreement with this form, with the values of R_c and ν which are quite close to the ones obtained by other methods.

On the other hand, it seems that the other two types of singularity discussed in [10] may be discarded, although they mimic power law in a limited range of r. Thus, for the Bray-Moore scaling ($\xi \sim e^{\tilde{a}/|R-R_c|^2}$, $R_c \sim 0$) experimental data lie on a noticeably concave curve (top inset in Fig. 6); the slope of its best-fit line, corresponding to the nonuniversal parameter $\tilde{a}$, manifests a systematic decrease as bigger and bigger systems (L) are added to the analysis. For the essential singularity ($\xi \sim e^{\tilde{b}/|R-R_c|}$, $R_c \sim 0.42$), which better agrees with our data, the shape of avalanche size distribution binned around H_c (bottom inset) varies smoothly around $R \sim 0.42$, but changes its curvature for $R = 0.54$.

In conclusion, we have demonstrated that the 2D nonequilibrium zero-temperature random field Ising model exhibits a critical behavior, which can be described by power-law scaling near the critical point. Our assertion is based on the results of numerical analysis of data collected in extensive simulations of systems which were sufficiently large to clearly display the critical behavior.

This work was supported by the Serbian Ministry of Science under Project No. 171027. We are grateful to the Scientific Computing Laboratory of the Institute of Physics in Belgrade for provided computer facilities and to one of our referees for bringing our attention to Ref. [14].

[1] D. P. Belanger and T. Nattermann, in *Spin Glasses and Random Fields*, edited by A. P. Young (World Scientific, Singapore, 1998).
[2] J. P. Sethna, K. A. Dahmen, and O. Perković, in *The Science of Hysteresis*, edited by G. Bertotti and I. Mayergoyz (Academic Press, Amsterdam, 2006).
[3] J. P. Sethna *et al.*, Phys. Rev. Lett. **70**, 3347 (1993).
[4] G. Durin and S. Zapperi, in *The Science of Hysteresis*, edited by G. Bertotti and I. Mayergoyz (Academic Press, Amsterdam, 2006); D. Spasojević, S. Bukvić, S. Milošević, and H. E. Stanley, Phys. Rev. E **54**, 2531 (1996).
[5] K. A. Dahmen and J. P. Sethna, Phys. Rev. Lett. **71**, 3222 (1993); Phys. Rev. B **53**, 14 872 (1996).
[6] O. Perković, K. A. Dahmen, and J. P. Sethna, Phys. Rev. Lett. **75**, 4528 (1995); Phys. Rev. B **59**, 6106 (1999).
[7] Also studied analytically—see D. Spasojević, S. Janićević, and M. Knežević, Europhys. Lett. **76**, 912 (2006).
[8] A. Maritan, M. Cieplak, M. R. Swift, and J. R. Banavar, Phys. Rev. Lett. **72**, 946 (1994); C. Frontera and E. Vives, Phys. Rev. E **59**, R1295 (1999); Phys. Rev. E **62**, 7470 (2000); A. K. Hartmann, Phys. Rev. B **65**, 174427 (2002); F. J. Pérez-Reche and E. Vives, Phys. Rev. B **67**, 134421 (2003); **70**, 214422 (2004); E. Vives, M. L. Rosinberg, and G. Tarjus, Phys. Rev. B **71**, 134424 (2005).
[9] Y. Liu and K. A. Dahmen, Europhys. Lett. **86**, 56003 (2009); Phys. Rev. E **79**, 061124 (2009).
[10] O. Perković, K. A. Dahmen, and J. P. Sethna, arXiv: cond-mat/9609072 v1.
[11] For a set of discrete curves we first find the union set $\mathcal{X}$ of all their ordinates, next for each x in $\mathcal{X}$ we find the (weighted) mean of the interpolated curves, and then the width around the mean curve, resulting in a merit function (i.e., width w) different from the one used in [12]. Various types of interpolation and weighted widths can be used, which is important for noisy data having different uncertainties. Here, we have employed the simplest choice—linear interpolation, no weights, and width $w = \sqrt{D_2/N}$, where D_2 is the sum of squared distances from the mean curve, and N is the number of degrees of freedom (crudely, the number of points in $\mathcal{X}$).
[12] S. M. Bhattacharjee and F. Seno, J. Phys. A **34**, 6375 (2001).
[13] W. H. Press, S. A. Teukolsky, W. T. Vetterling, and B. P. Flannery, *Numerical Recipes: The Art of Scientific Computing* (Cambridge University Press, Cambridge, 2007), 3rd ed.
[14] E. T. Seppälä, V. Petäjä, and M. J. Alava, Phys. Rev. E **58**, R5217 (1998).